Critical Josephson current in the dynamical Coulomb blockade regime

Berthold Jäck,[1,][*] Matthias Eltschka,[1] Maximilian Assig,[1] Markus Etzkorn,[1] Christian R. Ast,[1] and Klaus Kern[1,2]

[1]*Max-Planck-Institut für Festkörperforschung, 70569 Stuttgart, Germany*

[2]*Institut de Physique de la Matière Condensée, Ecole Polytechnique Fédérale de Lausanne, 1015 Lausanne, Switzerland*

The current-voltage characteristics of a voltage-biased Josephson junction in the low conductance regime of an ultra-low temperature scanning tunneling microscope (STM) is dominated by sequential charge tunneling. Using $P(E)$ theory we show that the Josephson coupling energy, experimentally determined in this regime, is in good agreement with the critical current I_0 calculated from the Ambegaokar-Baratoff formula. In this way, we can determine the critical current values of a Josephson junction in an STM. Furthermore, we experimentally determine a range of validity for $P(E)$ theory, which is in accordance with theoretical predictions. In this way, we establish an optimal parameter range, in which Josephson STM can be performed.

The DC Josephson effect describes the dissipationless tunneling of Cooper pairs between two superconducting electrodes, which manifests itself as a finite tunneling current at zero voltage [1]. The maximum amplitude of this current, the critical Josephson current I_0, directly depends on the normal state conductance G_N of the tunnel contact and the superconducting order parameters Δ_1 and Δ_2 of the two electrodes [2]. Thus, I_0 provides direct access to the superconductor's properties. Knowledge of the spatial variations in the superconducting order parameter Δ gives insight on the interaction of a superconductor with single magnetic impurities [3,4]. In addition, I_0 provides valuable information about the pairing symmetry of Δ in unconventional superconductors [5,6]. Therefore, the Josephson effect holds promising potential in combination with the nanoscale resolution of low temperature scanning tunneling microscopy (STM), where it is also referred to as Josephson STM (JSTM) [5]. In first JSTM experiments the tunneling of Cooper pairs through the atomic scale tunnel junction was demonstrated [7–10], and the spatial mapping of this current was also successfully realized [11]. Determining quantitative values of I_0 from JSTM experiments, however, has not been achieved so far, although this capability is of fundamental importance for the concept of JSTM [5]. One possibility to extract I_0 from experimental data is given by the Ivanchenko and Zil'berman model [12,13], if the capacitance can be neglected. However, in a typical STM geometry, the junction capacitance cannot be neglected [14]. Under these conditions, the so-called $P(E)$ theory [15,16] has to be used to describe the tunneling current. This has been demonstrated before both in the context of single-particle tunneling [17,18] as well as sequential Cooper pair tunneling [14].

In this Rapid Communication, we show that the local value of the critical Josephson current extracted from the fits of the $P(E)$ theory to the experimental data measured with an STM is in good agreement with the value from the Ambegaokar-Baratoff (AB) formula [2]. Further, we experimentally observe a regime in which the phase tunneling starts to dominate the sequential Cooper pair tunneling. In this way, we experimentally determine the range of pure sequential Cooper pair tunneling and thus the range of validity

of $P(E)$ theory. In the context of JSTM, this result also allows us to establish an optimal parameter range, in which JSTM experiments can be performed.

The current-voltage-characteristics of a Josephson junction generally depend on a number of different parameters, which requires a careful choice of the theoretical model [12,15,16]. To do this, we compare the different energy scales of all involved physical phenomena. These are the Josephson coupling energy $E_J = \hbar I_0/(2e)$ [$\hbar$ is the reduced Planck constant $\hbar = h/(2\pi)$ and e is the elementary charge], the Coulomb charging energy of the tunnel contact $E_C = 2e^2/C_J$, where C_J is the junction capacitance, as well as the thermal energy $E_T = k_B T$, where T is the temperature and k_B is the Boltzmann constant. The Josephson energy E_J in our case is on the order of 10 μeV, in the tunneling regime where $G_N \ll G_0$ (G_N is the normal state conductance and $G_0 = 2e^2/h$ denotes the quantum of conductance). The Coulomb charging energy E_C is on the order of 100 μeV assuming a typical STM junction capacitance C_J of a few femtofarad. At an effective temperature of 40 mK, the thermal energy E_T is 3.45 μeV [19].

Figure 1(a) compares these energy scales for different values of G_N [20]. We find that in the tunnel regime ($G_N \ll G_0$), the energy scales order in the following way: $E_T \ll E_J \ll E_C$. In particular, this means that the condition $E_T \leqslant E_J$ for JSTM to work best is fulfilled for most of the tunnel conductance range [5,12]. In addition, in the limit $E_J \ll E_C$, the tunneling current is created by the sequential tunneling of Cooper pairs, also referred to as the dynamical Coulomb blockade (DCB) regime. In this regime, the Cooper pairs tunnel inelastically releasing energy quanta $h\nu$ proportional to the junction bias voltage $V_J = h\nu/(2e)$ into the environment. The emitted photon spectrum has recently been studied in more detail [21], also in the context of nonlinear quantum dynamics [22]. The sequential Cooper pair tunneling characteristics can be modeled by the $P(E)$ theory [15,16], which treats the Josephson coupling energy E_J as a perturbation to the Coulomb energy E_C. This theory facilitates the determination of an experimental Josephson coupling energy E_J, which can be directly converted to the Josephson critical current $I_0 = (2e/\hbar)E_J$—giving access to Δ [15,16]. However, it is *a priori* not clear that the experimental values for I_0 found in the DCB regime correspond to the actual AB critical current that has been evaluated for the phase-tunneling regime
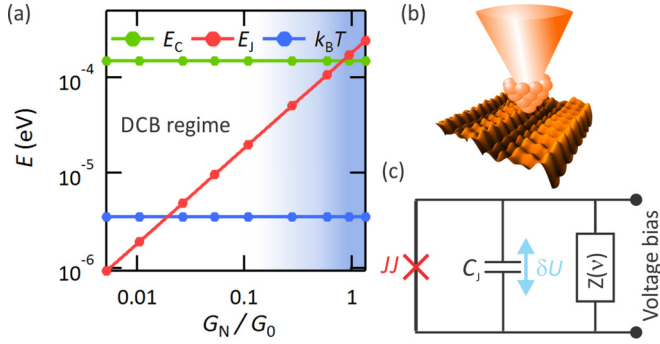
———————
[*]Corresponding author: berthold.jack@alumni.epfl.ch

FIG. 1. (a) Coulomb charging energy E_C, Josephson coupling energy E_J, and thermal energy E_T at $T_{eff} = 40$ mK versus normalized tunnel conductance G_N/G_0. E_C was calculated using the average capacitance value from the $P(E)$ fits. (b) Vanadium-vacuum-vanadium tunnel junction in the STM: The topography shows the (5×1) reconstructed V(100) surface measured at a setpoint of $V' = 2$ mV and $I = 5$ nA. Above the sample, an artistic view of the STM tip is shown. (c) Simplified circuit diagram of the experimental setup: JJ represents the Josephson junction, C_J the junction capacitance, δU the voltage noise, and $Z(\nu)$ the frequency-dependent environmental impedance.

[2,23]. Moreover, when the Josephson coupling energy E_J becomes comparable to E_C—in our case when $G_N \approx G_0$ [see Fig. 1(a)]—the Josephson junction enters a regime where phase tunneling becomes more and more dominant. Therefore, $P(E)$ theory, describing sequential Cooper pair tunneling, should fail to describe $I(V)$ characteristics measured in this regime, which remains an unresolved question until now.

We performed experiments on voltage-biased vanadium-vacuum-vanadium tunnel junctions using an STM at a temperature of $T = 15$ mK [19]. For the STM tip, we cut a polycrystalline V wire of 99.8% purity under tension (diameter $d = 250$ μm). The tip was prepared *in situ* by field-emission and voltage-pulses. The sample is a $V(001)$ single crystal [24,25], which has been prepared by cycles of sputtering and annealing to $T = 800 \,^\circ$C, as shown in Fig. 1(b). The normal state tunnel conductance $G_N = I_T/V_T$ is determined by the tunneling current I_T at a bias voltage reference V_T, where $eV_T \gg \Delta_1 + \Delta_2$. We correct the voltage axis for voltage drops over an effective circuit resistance R_{DC}, according to $V = V' - I(V')R_{DC}$ [26]. The primed and unprimed voltages denote the applied bias voltage and the junction bias voltage, respectively.

The perturbative approach of $P(E)$ theory applies Fermi's golden rule to calculate the tunneling current [27]:

$$I(V) = \frac{\pi e}{\hbar} E_J^2 [P(2eV) - P(-2eV)], \qquad (1)$$

where $P(E)$ is the spectral probability for a tunneling Cooper pair to emit ($E > 0$) or absorb ($E < 0$) a photon to or from the environment. The probability distribution $P(E)$ is only determined by the electromagnetic environment $Z(\nu)$ of the junction and independent of the normal state conductance G_N [15,16]. The Josephson effect enters *only* through the scaling factor E_J^2, which is particularly advantageous for the following data analysis: $I(V)$ curves measured at different values of G_N can be modeled by the *same* $P(E)$ function scaled by E_J^2. We
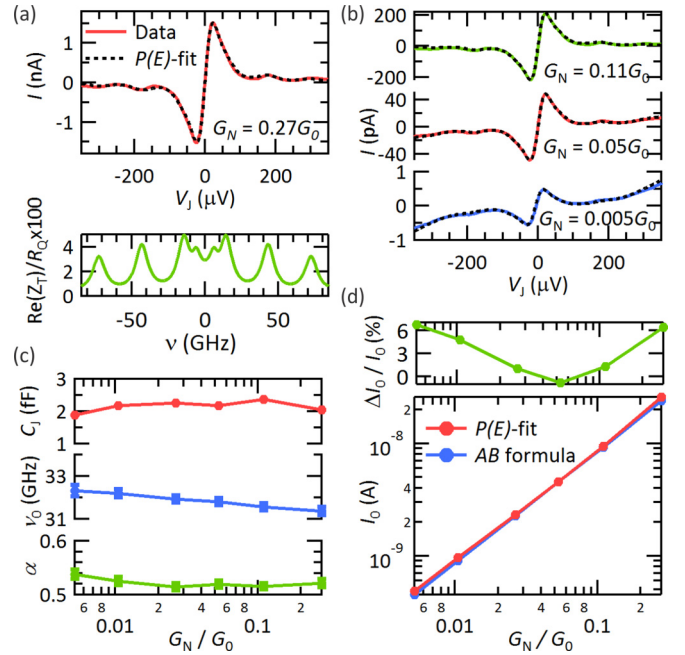

FIG. 2. (a) Typical $I(V)$ curve and the corresponding $P(E)$ fit. On the bottom the real part of $Z_T(\nu)$ normalized to the quantum of resistance $R_Q = h/2e^2$ is shown (cf. Refs. [14] and [30]). (b) $I(V)$ curves measured at selected tunnel conductances G_N. The $P(E)$ fits are shown as dashed black lines. (c) Fitted capacitance values C_J as well as impedance parameters ν_n and α as function of G_N/G_0. (d) Experimentally determined [$P(E)$ fit] and calculated values (AB formula) of the critical current as well as their relative deviation $\Delta I_0/I_0$ as a function of G_N/G_0. The error bars are within the size of the symbols.

will use this property later to mark the range of validity of $P(E)$ theory. E_J is independent of $Z(\nu)$, for which reason its value can be unambiguously determined with high precision. The probability $P(E)$ in Eq. (1), whose energy integral normalizes to one, is a convolution of two independent energy exchange probabilities $P_Z(E)$ and $P_C(E)$ [27–29]. The probability $P_Z(E)$ describes the energy exchange with the immediate environment, which is characterized by a complex, frequency dependent impedance $Z_T(\nu)$. In the STM, this comprises the junction capacitance C_J as well as the tip, which acts as a $\lambda/4$-monopole antenna. It can be modeled effectively by a modified open-ended transmission line impedance [14,30], whose real part is displayed in Fig. 2(a). Moreover, phase diffusion effects due to finite temperature in the resistive leads are incorporated in $P_Z(E)$ through an ohmic contribution $R = Z_T(0)$ at zero frequency. The second distribution $P_C(E)$ accounts for an experimentally observed broadening of the Cooper pair current spectrum. A likely source of this broadening is thermal charge fluctuations in the junction electrodes resulting in thermal voltage fluctuations δU across the junction capacitance. We estimate the corresponding $P_C(E)$ function to be of Gaussian shape with a standard deviation of $\sigma = \sqrt{2E_C k_B T}$ [29,31]. We will show in the following that the contribution from the thermal voltage fluctuations is essential for modeling the $I(V)$ curves.

A typical $I(V)$ curve measured at a conductance of $G_N = 0.27\,G_0$ is shown in Fig. 2(a). The $I(V)$ curve features a dominant supercurrent peak near zero voltage and well-defined spectral resonances at higher voltages, which originate from the interaction of the junction with the tip-assembly impedance [14,15,32]. Moreover, in comparison with previous studies, e.g., Refs. [13] and [32], all current features exhibit a rather broad contour, which can be attributed to the intrinsically low quality factor of antennas as well as the impact of the voltage fluctuations δU. The challenge in fitting an $I(V)$ curve using $P(E)$ theory lies in the rather complex interplay of the different fitting parameters. Therefore, the experimental parameters require more detailed consideration. The resistive junction leads are transmission lines, for which reason we can set the dissipative impedance at zero frequency $Z_T(0)$ to the input impedance of a transmission line, $R = 377\,\Omega$ [33]. We use an effective electronic temperature of $T_{\mathrm{eff}} = 40$ mK, which is slightly higher than the base temperature of our system, as we can not perfectly shield it from stray photons—a result from operating an STM [19].

Incorporating these assumptions, we can fit the experimental $I(V)$ curve at $G_N = 0.27\,G_0$ as shown in Fig. 2(a). The fit nicely reproduces both the supercurrent peak as well as the spectral resonances, and we can extract a Josephson coupling energy of $E_J = 52.69 \pm 0.53\,\mu$eV. The environmental impedance $Z_T(\nu)$ shows its base resonance frequency at $\nu_0 = 31.34 \pm 0.04$ GHz, and a corresponding damping factor $\alpha = 0.52 \pm 0.01$ (cf. Ref. [14]). For the junction capacitance, we find a typical value of $C_J = 2.04 \pm 0.07$ fF. We conclude that the $I(V)$ curves from our small capacitance tunnel junction showing the characteristics of Cooper pair tunneling can be nicely modeled by $P(E)$ theory with reasonable parameters that are independently reproducible. Moreover, we are able to unambiguously determine an experimental value of the Josephson coupling energy E_J in a particular junction.

We have repeated the same analysis for several Cooper pair tunneling characteristics over a large range of the normal state tunneling conductance $0.0052\,G_0 \leqslant G_N \leqslant 1.35\,G_0$. The measured $I(V)$ curves were fitted with $P(E)$ theory in the same fashion as before, of which three examples are shown in Fig. 2(b). For all values of G_N, $P(E)$ theory nicely describes the tunneling current. As expected, the fitted values for the junction capacity C_J and the environmental impedance $Z(\nu)$ do not depend on G_N, as shown in Fig. 2(c). These results corroborate the consistency of our $P(E)$ implementation and fitting routine. From the fitted Josephson coupling energy E_J, we can directly calculate an experimental critical current $I_0 = 2e/\hbar E_J$. Its dependence on the normal state tunneling conductance G_N is displayed in Fig. 2(d). We find that I_0 linearly depends on G_N over almost two orders of magnitude for $G_N \leqslant 0.27 G_0$. We will show below that $P(E)$ theory breaks down for $G_N \geqslant 0.59 G_0$. As underlined above, the $P(E)$ distribution is independent of G_N [cf. Eq. (1)]. Hence, we can assign this linear increase of I_0 entirely to the increase of G_N, which is in agreement with the AB formula [2].

To quantitatively compare the experimentally found values for the critical current with the critical current values calculated from the AB formula, we write the AB formula for two superconductors with unequal order parameters $\Delta_{1,2}$ and
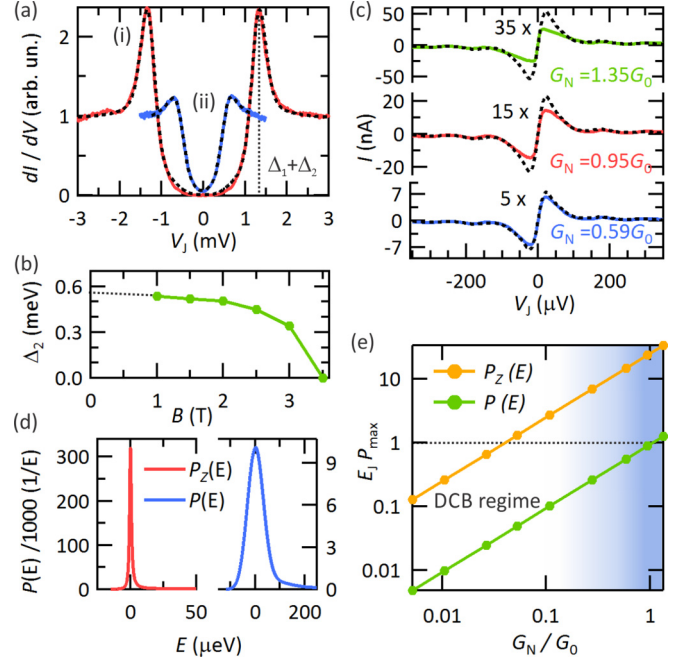

FIG. 3. (a) dI/dV spectra of the tunneling current (colored lines) and the corresponding fits (dashed lines) at zero magnetic field (i) and at 1 T, where the sample is normal conducting (ii). The spectra were recorded at $G_N = 0.003 G_0$ using standard lock-in techniques at a modulation frequency of $f_{\mathrm{mod}} = 720$ Hz and an amplitude of $V_{\mathrm{mod}} = 20\,\mu$V. (b) Dependence of the tip gap Δ_2, as extracted from the Maki fits, as a function of the externally applied magnetic field B. The extrapolation to zero magnetic field is indicated by the dashed line. (c) $I(V)$ curves (colored lines) and upscaled fits (dashed black lines) measured at large values of G_N. The scaling factors with respect to the fit at $G_N = 0.27\,G_0$ are indicated. (d) Calculated probability distribution $P_Z(E)$, only considering the dissipative environment, and the total distribution $P(E)$ that also considers the capacitive voltage noise δU. Note the different scales in the two panels. (e) The products $E_J P_{Z,\,\mathrm{max}}$ and $E_J P_{\mathrm{max}}$ as a function of the normalized conductance G_N/G_0 indicating the range of validity of $P(E)$ theory.

$\Delta_1 > \Delta_2$ [2]:

$$I_0 = \Delta_2 G_N\ K\left(\sqrt{1 - \frac{\Delta_2^2}{\Delta_1^2}}\right). \qquad (2)$$

Here, K denotes Jacobi's full elliptic integral of the first kind. We can independently determine the sample gap Δ_1 and the tip gap Δ_2 by measuring the quasiparticle excitation spectra as a function of the magnetic field shown in Fig. 3. The sample becomes normal conducting at $B_{c,2} = 0.5$ T [24], but the tip has a much larger critical field due to the confined geometry at the apex [34]. We, therefore, extract the tip gap using a Maki model fit for higher fields shown in Fig. 3(b) [35]. Extrapolating to zero field, we find a tip gap of $\Delta_2 = 563 \pm 20\,\mu$eV [36]. The sample gap Δ_1 we can extract from a Dynes fit to the zero field spectrum having the value $\Delta_1 = |\Delta_1 + \Delta_2| - \Delta_2 = 748 \pm 25\,\mu$eV, as shown in Fig. 2(a) [37–39]. The reduction of the tip gap compared to the bulk value is common in vanadium tips [35] and may be explained by the influence of vanadium oxide at the tip surface, changes in the phonon dispersion, or grain size effects [24,40–42]. Inserting these values along with

G_N into the AB formula, we can plot the corresponding critical currents in Figure 2(d) as a function of G_N. The critical currents from the $P(E)$ fit and the AB formula match within <7% [cf. upper panel in Fig. 2(d)] over the entire range of conductance. This is a remarkable observation, because the experimental values were determined in the DCB regime, whereas the AB formula was derived in the phase-tunneling regime. Our findings confirm the established interpretation of the critical current I_0 as a coupling strength between the overlapping pair wave functions, which is independent of the actual tunneling process [2].

We further tested the range of validity of $P(E)$ theory in the limit $E_J \rightarrow E_C$. Here the initial requirement of this perturbative approach $E_J \ll E_C$ is no longer valid so that $P(E)$ theory should break down. However, Ingold *et al.* found that the global condition $E_J \ll E_C$ is superimposed by another condition $E_J P(E) \ll 1$ [29]. This condition means essentially that sequential tunneling holds as long as the tunneling probability is low enough. In order to test this hypothesis, we measured the $I(V)$ curves for values of the normal state tunneling conductance $G_N \geqslant 0.59\ G_0$ of which three examples are shown in Fig. 3(b). Using $P(E)$ theory as before, we were unable to properly fit any of these $I(V)$ curves, which is to be expected, since at the measured conductance values, we find $E_J \approx E_C$ [cf. Fig. 1(a)]. Nevertheless, we can upscale a fitted current spectrum from experiments at a lower conductance $G_N = 0.27\ G_0$. The upscaled $I(V)$ curve nicely fits the spectral resonances at higher voltages but largely overestimates the supercurrent peak in all cases with increasing mismatch for higher values of G_N, as shown in Fig. 3(b), indicating the breakdown of $P(E)$ theory.

To better understand this observation, we investigated the product $E_J P_{max}$, where P_{max} is the global maximum of $P(E)$. It is found at zero voltage for the probability distribution of the impedance $P_Z(E)$ as well as the total, convoluted probability distribution $P(E)$ [see Fig. 3(c)] [29]. It can be seen that the broadening of the total $P(E)$ due to the capacitive noise greatly reduces the maximum value of $P(E)$ compared to $P_Z(E)$. The dependence of $E_J P_{max}$ on the tunnel conductance G_N is shown in Fig. 3(d). For a conductance of $G_N \geqslant 0.59\ G_0$, we find $E_J P_{max} \geqslant 1$ so that the required condition for $P(E)$ theory is "locally" violated near zero voltage. This result perfectly explains our observation that $P(E)$ theory fails to describe the

supercurrent peak close to zero bias voltage, where $P(E)$ has its maximum and $E_J P(E \approx 0) \approx 1$. Therefore, we observe phase tunneling at low voltages and charge tunneling at higher voltages in the same spectrum and, thus, $P(E)$ theory fails to model the entire $I(V)$ curve. For quantitative agreement with the experimental data in this regime, higher order perturbation theory may have to be taken into account (see, e.g., Ref. [43]).

Moreover, fitting the $P(E)$ function to our data reveals the significance of the thermal voltage fluctuations as a spectral broadening mechanism. While the probability distribution in the convoluted $P(E)$ function is broadened and has some spectral weight at higher voltages, the $P_Z(E)$ distribution—only containing the interaction with the dissipative environment— sharply peaks at $V = 0$ [see Fig. 3(c)]. For this reason, the required condition $E_J P_{Z,\ max} \ll 1$ is violated for almost the entire conductance range as shown in Fig. 3(d). This is in agreement with theory, since we operate the junction in a low impedance environment [i.e., $Z(0) \ll 1/(2\ G_0)$]. Therefore, thermal voltage fluctuations have to be included [29,31] to correctly describe our data. This reduces the P_{max} values and results in an overall consistent picture between experiment and theory as well as the range of validity.

In summary, we have investigated the $I(V)$ characteristics of a voltage-biased Josephson junction in the DCB regime with an STM. We found that the experimentally determined values for the critical current $I_0 = 2e/\hbar E_J$ in the DCB regime are in good agreement with the theoretical values calculated by the AB formula within a deviation of less than 7%. The DCB regime, which is predominantly accessible in STM, can, therefore, be used to determine the critical current I_0 of the Josephson junction. Thus, with precise tuning of the involved energy scales (E_T, E_J, E_C), we can operate our STM in the optimal JSTM regime. Furthermore, we could experimentally define the range of validity for pure sequential Cooper pair tunneling in which $P(E)$ theory can be applied. Our results represent the fundamental step towards the implementation of JSTM as a versatile spectroscopic tool for studying superconducting properties on the atomic scale [3–5] and further allow us to shed more light on the transition between sequential Cooper pair and coherent phase tunneling.

---

[1] B. D. Josephson, Phys. Lett. **1**, 251 (1962).

[2] V. Ambegaokar and A. Baratoff, Phys. Rev. Lett. **10**, 486 (1963).

[3] M. H. Flatté and J. M. Byers, Phys. Rev. Lett. **78**, 3761 (1997).

[4] M. I. Salkola, A. V. Balatsky, and J. R. Schrieffer, Phys. Rev. B **55**, 12648 (1997).

[5] J. Smakov, I. Martin, and A. V. Balatsky, Phys. Rev. B **64**, 212506 (2001).

[6] D. J. Van Harlingen, Rev. Mod. Phys. **67**, 515 (1995).

[7] O. Naaman, W. Teizer, and R. Dynes, Phys. Rev. Lett. **87**, 097004 (2001).

[8] J. G. Rodrigo, V. Crespo, and S. Vieira, Phys. C (Amsterdam, Neth.) **437–438**, 270 (2006).

[9] N. Bergeal, Y. Noat, T. Cren, Th. Proslier, V. Dubost, F. Debontridder, A. Zimmers, D. Roditchev, W. Sacks, and J. Marcus, Phys. Rev. B **78**, 140507(R) (2008).

[10] H. Kimura, R. P. Barber, Jr., S. Ono, Y. Ando, and R. C. Dynes, Phys. Rev. Lett. **101**, 037002 (2008).

[11] Th. Proslier, A. Kohen, Y. Noat, T. Cren, D. Roditchev, and W. Sacks, Europhys. Lett. **73**, 962 (2006).

[12] Y. M. Ivanchenko and L. A. Zil'berman, Zh. Eksp. Teor. Fiz. **55**, 2395 (1968) [Sov. Phys. JETP **28**, 1272 (1969)].

[13] A. Steinbach, P. Joyez, A. Cottet, D. Esteve, M. H. Devoret, M. E. Huber, and J. M. Martinis, Phys. Rev. Lett. **87**, 137003 (2001).

[14] B. Jäck, M. Eltschka, M. Assig, A. Hardock, M. Etkorn, C. R. Ast, and K. Kern, Appl. Phys. Lett. **106**, 013109 (2015).

[15] M. H. Devoret, D. Esteve, H. Grabert, G.-L. Ingold, H. Pothier, and C. Urbina, Phys. Rev. Lett. **64**, 1824 (1990).

[16] D. V. Averin, Y. V. Nazarov, and A. A. Odintsov, Phys. B (Amsterdam, Neth.) **165–166**, 945 (1990).

[17] C. Brun, K. H. Müller, I-Po Hong, F. Patthey, C. Flindt, and W.-D. Schneider, Phys. Rev. Lett. **108**, 126802 (2012).

[18] L. Serrier-Garcia, J. C. Cuevas, T. Cren, C. Brun, V. Cherkez, F. Debontridder, D. Fokin, F. S. Bergeret, and D. Roditchev, Phys. Rev. Lett. **110**, 157003 (2013).

[19] Maximilian Assig, Markus Etzkorn, Axel Enders, Wolfgang Stiepany, Christian R. Ast, and Klaus Kern, Rev. Sci. Instr. **84**, 033903 (2013).

[20] While G_N can be tuned by changing the tip-sample distance, C_J remains unchanged, because the whole tip contributes to the capacitance on a macroscopic scale and not just a small part at the apex.

[21] M. Hofheinz, F. Portier, Q. Baudouin, P. Joyez, D. Vion, P. Bertet, P. Roche, and D. Esteve, Phys. Rev. Lett. **106**, 217005 (2011).

[22] V. Gramich, B. Kubala, S. Rohrer, and J. Ankerhold, Phys. Rev. Lett. **111**, 247002 (2013).

[23] P. Joyez, Phys. Rev. Lett **110**, 217003 (2013).

[24] S. T. Sekula and R. H. Kernohan, Phys. Rev. B **5**, 904 (1972).

[25] P. W. Davies and R. M. Lambert, Surf. Sci. **107**, 391 (1981).

[26] The in-line DC resistance of our setup R_{DC} contains experimentally determined contributions from the leads, low pass filters, as well as the input impedance of the current amplifier, which depends on the chosen amplification: $R_{DC} = 14\text{k}\Omega$ for $G_N \leqslant 0.026G_0$, $R_{DC} = 4.8\text{k}\Omega$ for $0.052G_0 \leqslant G_N \leqslant 0.27G_0$, and $R_{DC} = 3.9\text{k}\Omega$ for $G_N \geqslant 0.59G_0$.

[27] G.-L. Ingold, H. Grabert, and U. Eberhardt, Phys. Rev. B **50**, 395 (1994).

[28] G.-L. Ingold and H. Grabert, Europhys. Lett. **14**, 371 (1991).

[29] G.-L. Ingold and Yu V. Nazarov in *Single Charge Tunneling*, Ch. 2, *NATO ASI Series B*, Vol. 294 (Plenum Press, New York, 1992), p. 22.

[30] See Supplemental Material at http://link.aps.org/supplemental/10.1103/PhysRevB.93.020504 for a more detailed description of the environmental impedance $Z_T(\nu)$.

[31] C. R. Ast, B. Jäck, J. Senkpiel, M. Eltschka, M. Etzkorn, J. Ankerhold, and K. Kern, arXiv:1510.08449.

[32] T. Holst, D. Esteve, C. Urbina, and M. H. Devoret, Phys. Rev. Lett. **73**, 25 (1994).

[33] P. Joyez, D. Vion, M. Götz, M. Devoret, and D. Esteve, J. Supercond. **12**, 757 (1999).

[34] R. Meservey, P. M. Tedrow, and P. Fulde, Phys. Rev. Lett. **25**, 1270 (1970).

[35] M. Eltschka, B. Jäck, M. Assig, O. V. Kondrashov, M. A. Skvortsov, M. Etzkorn, C. R. Ast, and K. Kern, Nano Lett. **14**, 7171 (2014).

[36] M. Eltschka, B. Jäck, M. Assig, O. V. Kondrashov, M. A. Skvortsov, M. Etzkorn, C. R. Ast, and K. Kern, Appl. Phys. Lett. **107**, 122601 (2015).

[37] R. C. Dynes, V. Narayanamurti, and J. P. Garno, Phys. Rev. Lett. **41**, 1509 (1978).

[38] T. M. Klapwijk, G. E. Blonder, and M. Tinkham, Physica **109–110**, 1657 (1982).

[39] M. Ternes, W.-D. Schneider, J.-C. Cuevas, C. P. Lutz, C. F. Hirjibehedin, and A. J. Heinrich, Phys. Rev. B **74**, 132501 (2006).

[40] W. L. McMillan, Phys. Rev. **167**, 331 (1968).

[41] T. T. Chen, J. T. Chen, J. D. Leslie, and H. J. T. Smith, Phys. Rev. Lett. **22**, 526 (1969).

[42] M. Strongin, R. S. Thompson, O. F. Kammerer, and J. E. Crow, Phys. Rev. B **1**, 1078 (1970).

[43] J. Leppäkangas, M. Fogelström, A. Grimm, M. Hofheinz, M. Marthaler, and G. Johansson, Phys. Rev. Lett. **115**, 027004 (2015).